Electron paramagnetic resonance of Ce^{3+} in strontium-barium niobate

2000 J. Phys.: Condens. Matter 12 4277

(http://iopscience.iop.org/0953-8984/12/18/312)

J. Phys.: Condens. Matter **12** (2000) 4277–4284. Printed in the UK PII: S0953-8984(00)06136-1

Electron paramagnetic resonance of Ce^{3+} in strontium–barium niobate

J Wingbermühle†, M Meyer†, O F Schirmer†, R Pankrath† and R K Kremer‡

† Fachbereich Physik, Universität Osnabrück, D-49069 Osnabrück, Germany
‡ Max-Planck-Institut für Festkörperforschung, D-70567 Stuttgart, Germany

E-mail: schirmer@uos.de

Received 20 July 1999, in final form 3 March 2000

Abstract. The EPR of Ce^{3+} in congruent $Sr_xBa_{1-x}Nb_2O_6$ ($x = 0.61$) is characterized by the orthorhombic g-tensor {0.89, 3.55, 0.54} with principal axes lying in the c-plane, tilted with respect to the a- and b-axes by 21.1°, and along the c-axis. Ce^{3+} occupies a single crystallographic site in the crystal, leading to a unique EPR spectrum. The point symmetry of the Ce^{3+} position, C_1, is lower than that of the replaced alkaline-earth ions, C_4 or C_s. This is attributed to an off-centre movement of Ce^{3+}. The Ce^{3+} signal decreases under illumination. No further EPR signal is detected to arise from the photoionization of Ce^{3+}.

1. Introduction

The incorporation of cerium into strontium–barium niobate crystals ($Sr_xBa_{1-x}Nb_2O_6$ (SBN), $0.25 \leqslant x \leqslant 0.75$) increases their photorefractive sensitivity [1]. In order to assess the role of cerium doping in this context and to possibly improve the performance of SBN:Ce, the structure of the cerium centre responsible and the corresponding light-induced charge-transfer processes must be known. Related studies have revealed that the primary step of the photorefractive effect in this material is the electron photoionization of Ce^{3+} to the conduction band, where the electrons are self-trapped, forming Nb^{4+} small polarons [2]. Both Ce^{3+} and Nb^{4+} are paramagnetic ions and could thus be studied, in principle, by electron paramagnetic resonance (EPR). A previous EPR investigation of SBN:Ce^{3+} has identified a signal, which was attributed to Ce^{3+} [3]. This signal did not show any angular dependence of the resonance fields when the angle of the static magnetic field was varied with respect to the crystal axes. This situation is quite unexpected and unlikely for Ce^{3+} in a crystal of low symmetry, such as SBN. In this paper we shall present a detailed EPR study of Ce^{3+} in SBN, demonstrating that this ion does indeed show a strong angular dependence of its resonance fields. The analysis of the data indicates that the Ce^{3+} EPR spectra originate from a single crystallographic position in the crystal. Resonances of Nb^{4+} have so far not been detected.

2. Crystal structure of SBN and its consequences for the EPR spectra of incorporated paramagnetic ions

SBN crystallizes in a tetragonal structure with the space group $P4bm$ [4]. The Nb^{5+} ions are surrounded by two types of distorted oxygen octahedron (B1 and B2) which are linked at

0953-8984/00/184277+08$30.00

their corners in such a way that channels are forming along the [001] direction (figure 1). The positions A1, favoured for Sr incorporation, and A2, occupied by Sr or Ba, lie on the axes of such channels at approximately $z = \frac{1}{2}c$, i.e. above or below the plane of figure 1, assumed to have $z = 0$; here c is the lattice constant along [001], 3.91 Å [4]. The channel C is empty.

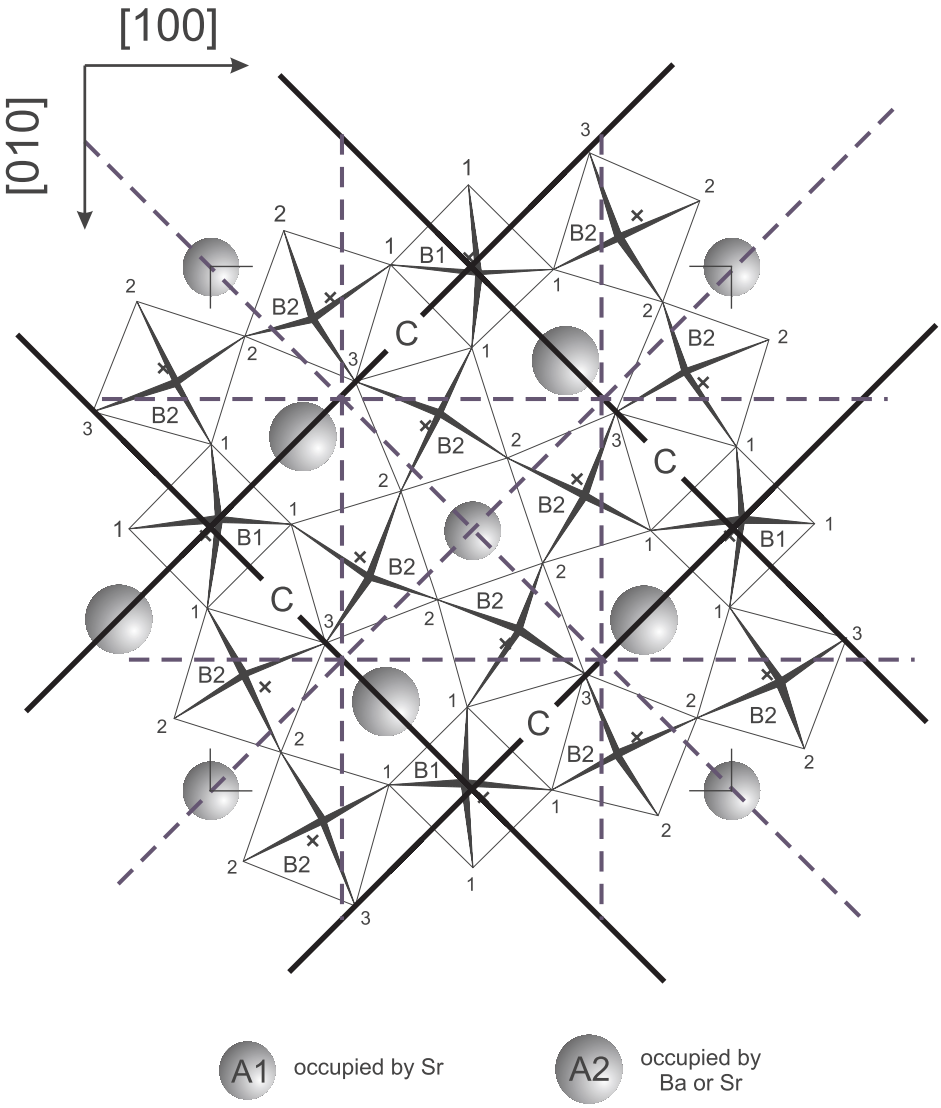

Figure 1. The structure of SBN as seen along the c-axis, [001]. The right angles at the four outer A1 sites delineate boundaries of the unit cell. The ionic positions and the symmetry elements are indicated: full lines mark the traces of mirror planes, dashed ones those of glide mirror planes. The designation A1 labels sites preferred by Sr, A2 those occupied by Ba or Sr. The sites C are empty in the ideal structure. B1 and B2 are the two types of Nb position. The numbers at the corners of the O^{2-} octahedra mark O^{2-} ions and their equivalences. The z-coordinates of the O^{2-} ions labelled 1, 2 and 3 as well as of the Nb ions B1 and B2 are close to zero; for details, see reference [4]. The other ions, Sr and Ba, at A1 or A2, as well as the O^{2-} ions at perspectively thickened apexes of the B1 and B2 octahedra, lie at approximately $\frac{1}{2}$ of the lattice constant c, 3.91 Å. The crosses mark oxygen positions at $-\frac{1}{2}c$ below the plane.

The A1 sites, twelvefold oxygen coordinated, have axial symmetry, C_4; an isolated paramagnetic ion at this position will thus exhibit axially symmetric EPR spectra, i.e. the resonance fields are independent of the azimuthal angle of the static magnetic field in the (001) plane. Paramagnetic ions at both A1 sites in the crystal thus cannot be distinguished magnetically. The A2 sites, on the other hand, surrounded by 15 oxygen ions, have only mirror symmetry, C_s. EPR spectra from paramagnetic ions at such sites should lead to an angular dependence described by orthorhombic coupling tensors with principal axes in and perpendicular to the mirror planes. Because these A2 sites are related to each other by the fourfold axial symmetry of the crystal structure, ions at such positions will thus be characterized by EPR spectra periodically repeating themselves if the azimuth is advanced by 90 degrees. Among these four A2 sites, two magnetically inequivalent species can be distinguished because magnetic fields $\boldsymbol{B}$ and $-\boldsymbol{B}$ lead to identical signals. The sites C, ninefold oxygen coordinated, also have mirror symmetry, C_s. It is unlikely that Ce^{3+} will replace the Nb ions at sites B1 and B2, since the available volume is too small there. Still it is worthwhile to discuss the structure of possible EPR spectra resulting from paramagnetic ions at such sites. B1 has symmetry C_s and thus again two sites can be distinguished magnetically. The lowest possible symmetry, C_1, is found at the B2 sites. Plots of the related angular dependences of the EPR spectra corresponding to the eight B2 sites will comprise four branches, taking into account the equivalence of the $\boldsymbol{B}$- and $-\boldsymbol{B}$-directions, i.e. four sites can be distinguished magnetically.

The unit cell of SBN contains five formula units. Therefore there are only five alkaline-earth ions to be distributed among the six A1 and A2 sites. One of these sites is then statistically unfilled. The local crystal fields at the ion sites in the crystal thus deviate from those expected for a regularly ordered crystal. They will vary locally depending on the distance to the unfilled sites. Such potential fluctuations are typical for crystals that are not regularly ordered, such as substoichiometric, i.e. Li-deficient $LiNbO_3$ [5].

3. Experimental details

The crystals investigated were grown by the Czochralski method at the Physics Department of the University of Osnabrück from a congruently melting ($x = 0.61$) SBN composition containing 0.4 weight per cent of CeO_2. For this doping of the melt the distribution coefficient of Ce in SBN is 0.74, as revealed by a neutron activation study [6]. XPS investigations [7] have shown that Ce is incorporated into SBN almost exclusively as Ce^{3+}, the Ce^{3+}/Ce^{4+} concentration ratio being 600. Crystals of typical sizes $3 \times 4 \times 5$ mm^3 have been used. EPR measurements were performed with a Bruker ER 200 D-SRC spectrometer near 9 GHz. Cooling was achieved with an Oxford ESR-900 helium-gas-flow cryostat. Most of the spectra were taken at 18 K.

4. Experimental results and their evaluation

The resonances to be attributed to Ce^{3+} can be observed below 40 K. At low temperatures the signals have deformed shapes characteristic for adiabatic fast-passage conditions. Normal line shapes are detected above about 15 K. But still some asymmetry remains (figure 2), also at higher temperatures, a feature which is similar to that for the signal shapes usually met for slightly disordered crystals, such as substoichiometric $LiNbO_3$ [5]. Here the asymmetry of the resonances was shown to be caused by local potential fluctuations resulting from the statistical occupations of lattice sites by defects related to the deviation from stoichiometry. Also in the present case the resonance fields of the EPR lines can therefore be determined only rather inaccurately. Only by fitting the systematic variations of the resonance positions

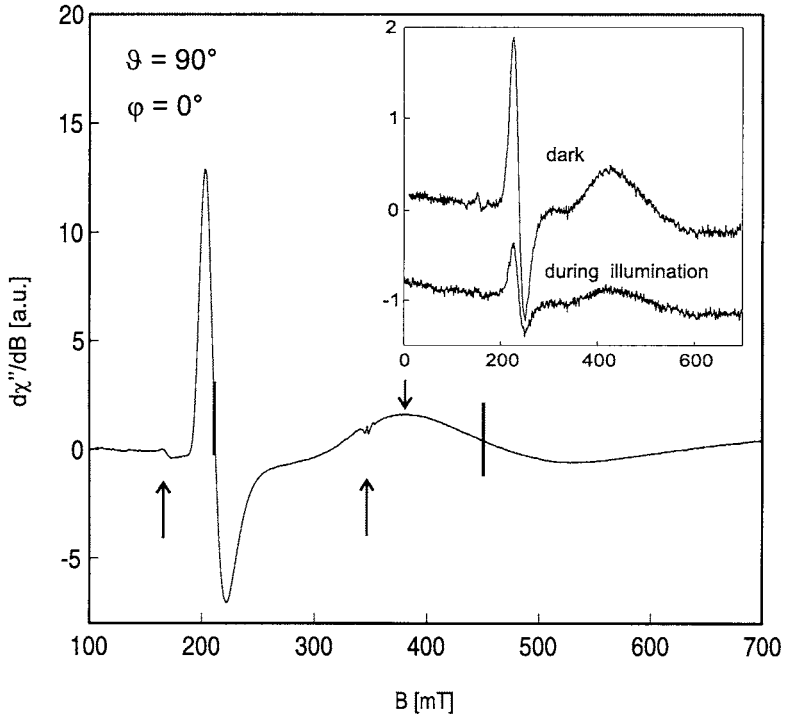

Figure 2. A typical EPR spectrum of Ce^{3+} in SBN for $\boldsymbol{B}$ in the (001) plane at an azimuthal angle $\varphi = 0°$. The lines indicated by long arrows mark resonances of Fe^{3+}, not investigated here. The vertical bars indicate the estimated positions of the EPR signals, as plotted in figure 3. It is seen that the maxima (short arrow) of the (derivative) EPR signals can be identified more accurately. Also these positions are given in figure 3, leading to a more precise value of the extremal line positions in the (001) plane. The inset demonstrates the decrease of the Ce^{3+} signals under illumination (here for $\lambda = 488$ nm with 0.1 W mm^{-2} intensity).

under rotations of the crystals with respect to the static magnetic field is a reliable analysis of the spin-Hamiltonian parameters achieved. Figure 3 displays an angular plot, where the azimuthal angle φ is varied in steps of two degrees. Especially at high magnetic fields, where the signals become rather wide, the resonance positions can be identified only with large error bars. More accurate is the identification of the resonance maxima, as indicated by a short arrow in figure 2 as an example. The angle at which the resonance fields pass through a maximum is determined rather precisely in this way to be $\varphi_0 = 21.1° \pm 0.5°$ with respect to the [100] or [010] directions.

The dependence of the resonance fields on the azimuthal angle (figure 3) contains four branches periodically displaced with respect to each other according to the scheme in figure 4. Here the directions of maximal resonance fields are indicated. They can be identified, see below, with principal directions of the respective g-tensors. The scheme demonstrates for instance that for $\boldsymbol{B}$ at $\varphi = 0°$ or at $\varphi = 45°$ only two lines are observed, because in each of these cases only two different angles between $\boldsymbol{B}$ and the principal directions occur. Further crossings appear for $\boldsymbol{B}$ along the medians between directions 4 and 2 or 1 and 3, respectively.

Before discussing the implications of the data presented in figure 3, the dependence of the spectra on the polar angle θ is demonstrated; see figure 5. In the centre part of this graph the dependence on φ is repeated. It is seen that the highest resonance fields are observed for

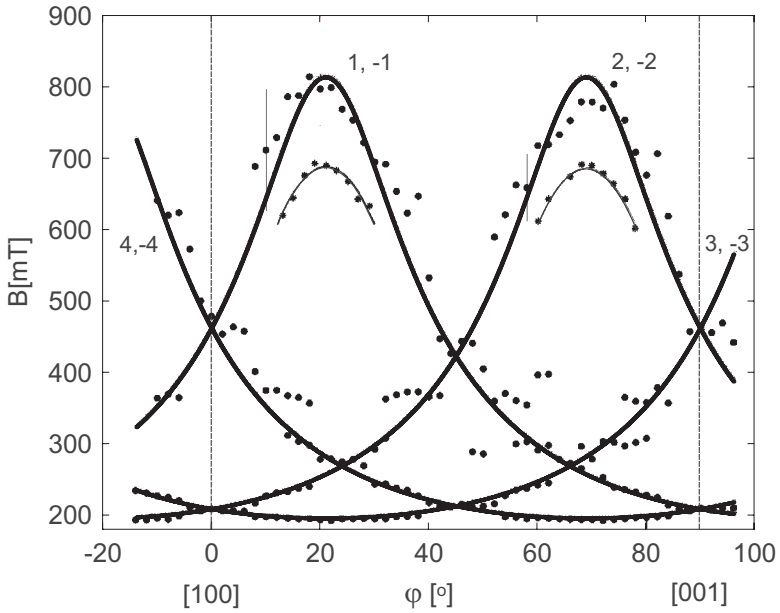

Figure 3. The angular dependence of the EPR line positions for variation of $\boldsymbol{B}$ in the (001) plane. The predicted positions, as based on a fit of the g-tensor components to all measured resonance fields, are indicated by the thick curves. The thin lines mark the angular dependence of the resonance maxima (see figure 2). The numbers in the plot attribute the four branches to the various centres distinguishable magnetically, as explained in figure 4.

$\boldsymbol{B}$ along the tetragonal direction, [001]. Here the uncertainties in the determination of the resonance fields are especially large.

The spin-Hamiltonian describing the angular dependence of the spectra is $H = \mu_B \boldsymbol{B}\mathbf{g}\boldsymbol{S}$ with $S = \frac{1}{2}$. Here S is an effective spin describing the twofold multiplicity of the lowest Kramers doublet of $Ce^{3+}(4f^1)$. It is separated from the next excited doublet by a crystal-field splitting, which for Ce^{3+} in low crystal-field symmetry is of the order of 100 cm^{-1} [8] and thus much larger than the microwave quantum, $\sim$0.3 cm^{-1}. The nuclear spin I of all stable Ce isotopes is zero, and therefore no hyperfine structure is expected. Fitting the components of the g-tensor to the observed field positions, figure 3 and figure 5, using the program package *R-SPECTR* developed by Grachev†, the following principal values and directions are obtained: $g_{[100]-\varphi_0} = 0.89 \pm 0.01$, $g_{[010]-\varphi_0} = 3.55 \pm 0.005$, $g_{[001]} = 0.54 \pm 0.01$. As indicated, the principal axes are lying, within the limits of error, along the [001] direction and within the (001) plane, tilted from the [100] and [010] axes by φ_0.

Under illumination, the EPR (see the inset of figure 2) and the (4f–5d) optical absorption band of Ce^{3+}, peaked at 2.5 eV, decrease, and a wide band near 0.8 eV increases. Because of its characteristic shape, the latter must be attributed to isolated small electron polarons, i.e. to conduction band electrons, self-trapped at Nb^{5+} to form Nb^{4+} [2]. The corresponding charge-transfer process is then the photoexcitation of an electron from Ce^{3+} to the conduction band, formed mainly from Nb orbitals. Although Nb^{4+} is paramagnetic and corresponding resonances of this ion have been identified [9, 10] e.g. in $LiNbO_3$, where it is surrounded, in a similar way to in the present situation, by a distorted octahedron of oxygen ions, no EPR of Nb^{4+} could so far be detected in illuminated SBN:Ce.

† The program package *R-SPECTR* by V G Grachev, c/o Fachbereich Physik, Universität Osnabrück, was used.

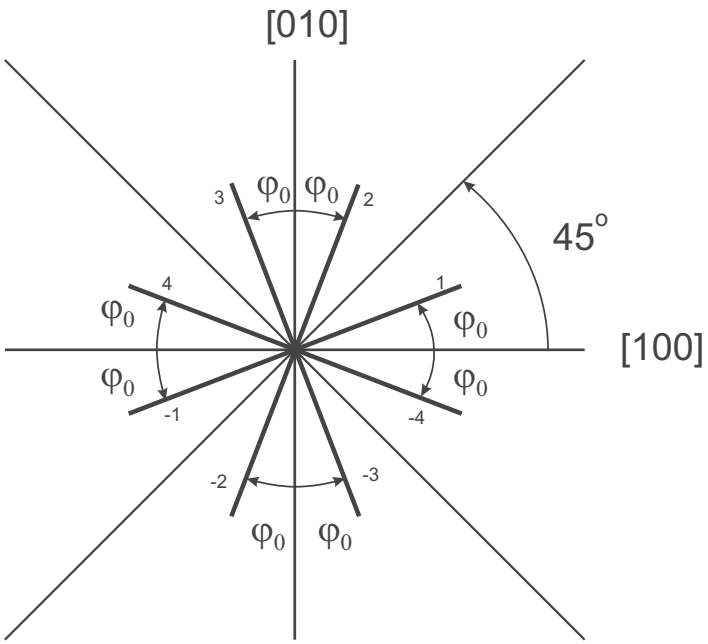

Figure 4. Angular positions of the g-tensor principal axes lying in the c-plane. The small numbers correspond to the labelling of the branches in figure 3.

5. Discussion

In principle, cerium can be incorporated into SBN at each of the cation sites, A1, A2, B1 and B2, and also at the structural vacancies, C. These alternatives have been taken into account in a shell-model analysis of the reactions describing the incorporation of Ce into SBN [11]. There it was predicted that Ce^{4+} is likely also to replace Nb at B1 or B2. This possibility is excluded for Ce^{3+} [11]. The different behaviour of the two charge states concerned can be traced to their different ionic radii: the radius of Ce^{3+} (100 pm) is much larger than that of Ce^{4+} (85 pm), which is closer to the radius of Nb^{5+} (70 pm). For both cerium charge states also doping at the structural vacancy site, C, is less likely than the competing reactions [11]. We are thus led to assume that Ce^{3+} sits at the A1 or A2 positions. This is in accord with conclusions based on the change of the Sr and Ba contents under increasing Ce concentrations, as concluded from a neutron activation analysis of the crystal compositions [6], where it was shown that Ce preferentially replaces Sr.

We have observed only one EPR spectrum characteristic for Ce^{3+}. Since a cerium ion at the A1 or A2 sites is surrounded by strongly differing arrangements of oxygen ions, it is unlikely that Ce^{3+} in these cases would lead to identical EPR spectra. Thus Ce^{3+} enters only at one of the possible sites. The same result was previously found by an XPS investigation [7]. So far we cannot, however, conclude which site is occupied by Ce^{3+}, because the observed symmetry is lower than those expected for both undistorted sites A1 and A2.

This statement is proved by the observation that the dependence of the Ce^{3+} spectra on azimuthal angle for $\theta = 90^\circ$ shows four symmetry-related branches, a feature expected only for sites of lower than mirror symmetry; see above. This could be attributed to the fact that Ce^{3+} creates for itself an environment at the possible sites A1 and A2 having a symmetry lower than C_s, i.e. symmetry C_1. Because Ce^{3+} is smaller than the replaced Sr or Ba ions (100 pm

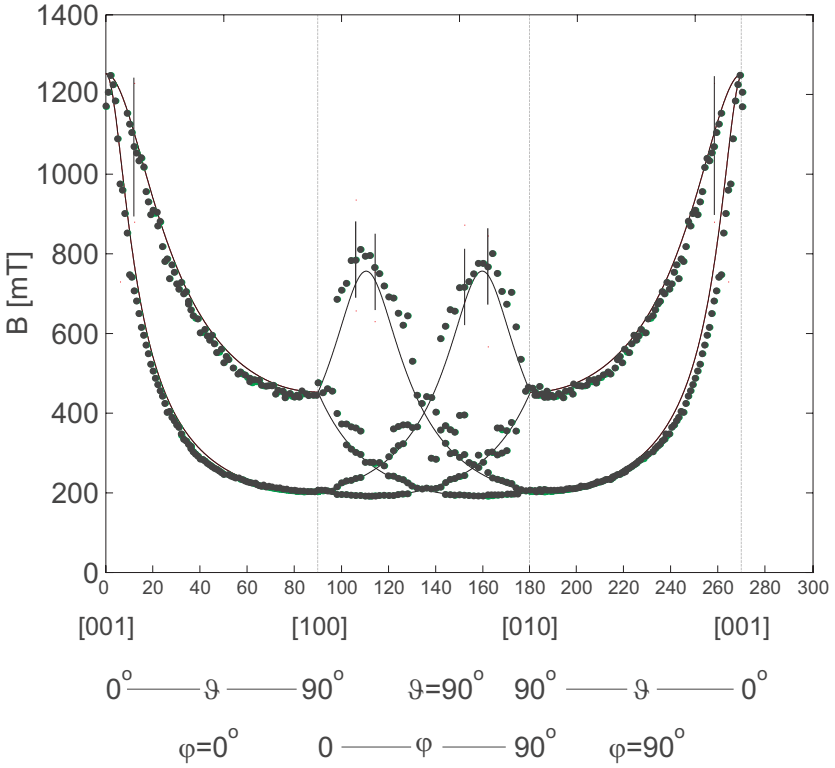

Figure 5. The total angular dependence of the Ce^{3+} resonance fields for the indicated variations of the magnetic field direction.

versus 118 pm and 135 pm, respectively), it can thus easily drift off-centre to a position of lower symmetry. This is especially the case for the A2 sites which are more spacious than the A1 sites (figure 2). Any such off-centre movement will have to occur in a direction perpendicular to the [001] axis. Only then can [001] be expected to be a principal direction of the g-tensor. Of course, an off-centre movement along this direction would also be consistent with a [001]-type principal axis. But in this case the observed EPR symmetry would have to be higher, i.e. either C_s (for Ce^{3+} on A2) or C_4 (for Ce^{3+} on A1).

It is rather unlikely that the low symmetry of the Ce^{3+} centre is caused by a close association with another, possibly compensating defect. This would require that such a lattice perturbation be found at a neighbouring O^{2-} site, since defects further away would be effectively screened by the O^{2-} ions next to Ce^{3+} and thus would not lead to crystal fields at Ce^{3+} strong enough to cause the pronounced symmetry reduction at this site to C_1. The influence arising from such a more distant compensation would tend to be as small as the effect of the statistically unoccupied A1 sites, leading to the slight asymmetry of the resonance signals.

This argumentation is consistent with the fact that the compensation of Ce^{3+}, charged onefold positively with respect to the replaced alkaline-earth ion, is unlikely to proceed by means of an ion in the next oxygen shell; such an ion would have to be negatively charged with respect to the replaced O^{2-}. Such replacements, by e.g. N^{3-} or P^{3-}, are chemically unexpected.

The compensation of Ce^{3+} will rather occur by means of cationic defects, i.e. by there being Nb^{4+} in the crystal ground state or additional alkaline-earth vacancies [11]. An also conceivable

compensation by extrinsic defects has been shown not to take place [6], the concentrations of suitable background impurities being too low [6]. The possibility of the presence of Nb^{4+} in the crystal ground state can be excluded, since the $Nb^{4+/5+}$ level forms the polaron ground state of the conduction band, lying higher than the Fermi level. This is pinned at the $Ce^{3+/4+}$ level, since these charge states coexist in the 'as-grown' SBN:Ce investigated [7]. The most likely compensation mechanism thus is the formation of alkaline-earth vacancies [7].

Our assignment of the reported resonances to Ce^{3+} is supported by comparison with EPR data on Ce^{3+} in other host crystals. Similar g-tensor components (3.162, 0.402, 0.395) as in the present case have, e.g., been observed for $YAlO_3$:Ce [12], where Ce^{3+} is also located at a site of low symmetry. Unfortunately, in such situations no further information can be derived from the EPR results, since the number of the relevant crystal-field parameters, from which the three g-tensor components could eventually be derived, is too high.

The photoionization of Ce^{3+} certainly leads to the creation of Nb^{4+} [2]. This charge state is in principle detectable by means of EPR; it has for instance been found in $LiNbO_3$ [9, 10]. So far one can only speculate as to why the corresponding resonances are not identified in the present case. We are inclined to attribute this lack of Nb^{4+} signals to excessive line broadening caused by strong spin–lattice coupling in the Nb^{4+} orbital ground state. Since the oxygen environments of Nb^{4+} deviate less from cubic symmetry than in $LiNbO_3$, there will be comparatively low-lying excited orbitals likely to cause short spin–lattice relaxation times by the combined action of spin–orbit and spin–lattice coupling.

Acknowledgments

We thank Dr G I Malovichko for reporting initial results, to Professor V G Grachev for helpful comments and to W Koslowski for support of the EPR Laboratory. This work was supported by DFG, Sonderforschungsbereich 225, *Oxide crystals for electro- und magnetooptical applications*.

References

[1] Megumi K, Kozuka H, Kobayashi M and Furuhata Y 1977 *Appl. Phys. Lett.* **30** 631
[2] Gao M, Pankrath R, Kapphan S and Vikhnin V 1999 *Appl. Phys.* B **68** 849
[3] Giles N C, Wolford J L, Edwards G J and Uhrin R 1995 *J. Appl. Phys.* **77** 976
[4] Jamieson P B, Abrahams S C and Bernstein J L 1968 *J. Chem. Phys.* **48** 5048
[5] Malovichko G I, Grachev V G, Kokanyan E P, Schirmer O F, Betzler K, Gather B, Jermann F, Klauer S, Schlarb U and Wöhlecke M 1993 *Appl. Phys.* A **56** 103
Malovichko G, Grachev V, Kokanyan E and Schirmer O 1999 *Phys. Rev.* B **59** 9113
[6] Woike T, Weckwerth G, Palme H and Pankrath R 1997 *Solid State Commun.* **102** 743
[7] Niemann R, Buse K, Pankrath R and Neumann M 1995 *Solid State Commun.* **98** 209
[8] Herrmann G F, Pearson J J, Wickersheim K A and Buchanan R A 1966 *J. Appl. Phys.* **37** 1312
[9] Faust B, Müller H and Schirmer O F 1994 *Ferroelectrics* **153** 297
[10] Müller H and Schirmer O F 1992 *Ferroelectrics* **125** 319
[11] Baetzold R C 1993 *Phys. Rev.* B **48** 5798
[12] Asatryan H R, Rosa J and Mares J A 1997 *Solid State Commun.* **104** 5